PERGAMON

International Journal of Solids and Structures 37 (2000) 2405–2428

INTERNATIONAL JOURNAL OF SOLIDS and STRUCTURES

www.elsevier.com/locate/ijsolstr

Modeling of compressive failure in fiber reinforced composites

K. Niu, R. Talreja*

School of Aerospace Engineering, Georgia Institute of Technology, Atlanta, GA 30332-0150, USA

Received 2 June 1998; in revised form 6 December 1998

Abstract

The classical results of compressive strength in fiber reinforced composites are briefly reviewed. The microbuckling analysis by Rosen (1965) and the Argon-Budiansky analysis for kink band formation (Argon, 1972; Budiansky 1983) are discussed and their results are rederived by using a new generalized Timoshenko beam model which is developed for a two-dimensional periodic matrix–fiber–matrix laminate. Introducing a 'shear hinge' to simulate a kink band and using the method of split rigidities it is shown that not only an initial fiber misalignment but also any misalignment in the loading system can affect the critical stress for kinking. A new mechanism based on shear instability of matrix is proposed for kink band formation and a simple formula is then derived to predict the kink band angle. Finally, a criterion for matrix yielding combining axial compressive stress and transverse shear perturbation is applied to modify the Argon–Budiansky kinking formula. © 2000 Published by Elsevier Science Ltd. All rights reserved.

1. Introduction

The compressive response of composite materials with long continuous fibers has been a subject of intense research over the past thirty years. It is well recognized that the compressive failure of these composites is usually caused by localized buckling of fibers. This failure process is referred to as microbuckling or kinking depending on the mode of local failure. Therefore, the study of this topic is divided into two branches: fiber microbuckling models (Rosen, 1965; Chung and Testa, 1968; Wang, 1978; Maewal, 1980; Hahn and Williams, 1986; Waas et al., 1990; Xu and Reifsnider, 1993, 1994; Tomblin et al., 1997, etc.) and kink band formation models (Argon, 1972; Budiansky, 1983; Steif, 1990; Budiansky and Fleck, 1993; Jensen and Christoffersen, 1997, etc.). Although some researches (Hahn and Williams, 1986; Chaudhuri, 1991) have shown that microbuckling and kink band type failure modes

* Corresponding author. Tel.: +1-404-894-1559; fax: +1-404-894-2760.
E-mail address: ramesh.talreja@aerospace.gatech.edu (R. Talreja)

PII: S0020-7683(99)00010-4

could be incorporated into one continuing theme, these two methods are still treated as parallel models (Schultheisz and Waas, 1996; Fleck, 1997).

A substantial body of experimental and theoretical results has enriched our knowledge of this topic. However some fundamental issues still remain open:

1. The well-known formula (Rosen, 1965) relating the critical stress for microbuckling to the axial shear modulus of a composite ($\sigma_1^c = G_{13}^c$) has not clearly been proven by a microbuckling analysis.
2. The Argon–Budiansky kink band analysis (Argon, 1972; Budiansky, 1983) can give a reasonable kinking stress estimate by introducing fiber misalignment of about 3° (Jelf and Fleck, 1992). However, as Deve (1997) has shown, realistic average misalignment angles are nearly zero. Some recent experimental observations (Schadler, 1998) seem to suggest that fiber misalignment may not even be necessary for the formation of kink bands.
3. Kink bands are experimentally observed to be inclined to the transverse direction (as recently reviewed by Schultheisz and Waas, 1996), and it is widely believed that a proper analysis of kink band angles is the key to understanding the kinking mechanism. The existing theories do not adequately predict the observed kink band angles.
4. Recent experiments (Soutis and Turkmen, 1995; Kyriakides et al., 1995; Daniel et al., 1996; Vogler and Kyriakides, 1997; Kyriakides and Ruff, 1997; Soutis, 1997; Moran and Shih, 1998) have shown that the axial compressive strain at the point of kink band formation is about 1%, which is of the same order of magnitude as a typical shear yield strain for a polymeric matrix. Therefore, it appears that the effect of the axial compressive stress on matrix yielding should be accounted for in the analysis of kink band formation.

The issues listed above will be addressed in this paper. The contents of the paper are organized as follows. In Section 2, a short literature review is given. In Section 3, a microbuckling approach is developed considering elastic bending and shear of the fibers and elastic shear of the matrix. This approach appears to be the first to apply the generalized Timoshenko beam theory to obtain the generalized Rosen formula. In Section 4, the initial transverse misalignment of fibers is introduced in the generalized Timoshenko beam model to bridge the microbuckling model and the Argon–Budiansky kink band model. In Section 5, a mechanism (called 'shear hinge' here) is proposed to give new interpretations to the Rosen and Argon–Budiansky formulas. In Section 6, a new theory of kink band formation based on an assumption of shear instability of matrix in compression is proposed and a simple expression for kink band angle is obtained which appears for the first time to give a reasonable prediction. In Section 7, the effect of axial compressive stress in matrix on kink band formation is discussed. Using a shear stress–strain relationship in the microbuckling model and applying the Tresca criterion a modified Argon–Budiansky kink band analysis is developed in which the kink band stress without fiber misalignment is included.

2. Review of microbuckling and kinking in composites

General reviews by Camponeschi (1991), Schultheisz and Waas (1996) and Fleck (1997) provide a large number of references to this subject. A brief review related to our topic is given below.

2.1. Microbuckling models

Rosen (1965) assumed two possible buckling modes: an extensional mode and a shear mode, as shown in Fig. 1. In composites of a significant fiber volume fraction, e.g., $v^f > 0.3$, the shear mode governs the compressive strength (Fleck, 1997). However, higher-order models (Chung and Testa, 1968; Zhang and

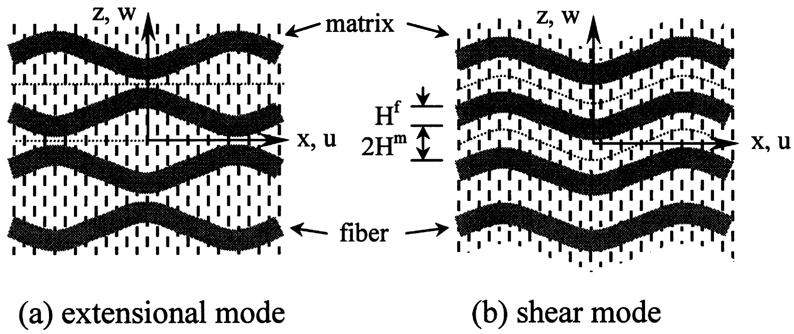

Fig. 1. Two modes in classical microbuckling analysis.

Latour, 1994) have shown that the shear mode is favored at all values of fiber volume fraction and the predictions of the two modes differ only slightly in the low fiber volume fraction range.

The compressive strength of composites with stiff fibers is given by Rosen (1965) as

$$\sigma_1^c = \frac{G^m}{1 - v^f} \tag{2.1}$$

where superscripts 'm', 'f' and 'c' refer to the matrix, fiber and composite, respectively. The Rosen result for the case of infinite fiber shear modulus can be written as

$$\sigma_1^c = G_{13}^c \tag{2.2}$$

As widely quoted (e.g., Fleck, 1997), the prediction by this expression is often several times higher than the experimental values. Many efforts have been made to modify Rosen's model by accounting for initial fiber misalignment, partial interfacial slippage and nonlinear shear stiffness (Wang, 1978; Hahn and Williams, 1986; Yeh and Teply, 1988; Stief, 1988; Chaudhuri, 1991; Sun and Jun, 1993; Xu and Reifsnider, 1993, 1994; Harberle and Matthews, 1994; Williams and Cairns, 1994; Chung and Weitsman, 1994, 1995; Tomblin et al., 1997).

2.2. Kink band formation models

Argon (1972) recognized that the initial fiber misalignment angle, ϕ_0, would have a large degrading effect on the compressive strength, and for a perfectly plastic composite having interlaminar shear strength, k, he showed that an additional rotation cannot develop until the critical compressive stress,

$$\sigma_1^c = \frac{k}{\phi_0} \tag{2.3}$$

is reached, which is independent of the volume fraction of the reinforcing element. Budiansky (1983) extended (without proof) Argon's expression to a more general expression that recovers Rosen's result as

$$\sigma_1^c = \frac{k^c}{\gamma_y^c + \phi_0} = \frac{G_{13}^c}{1 + \phi_0/\gamma_y^c} \tag{2.4}$$

where k^c is the shear yield stress of the composite, and the yield strain is defined as $\gamma_y^c = k^c/G_{13}^c$. Budiansky and Fleck (1993) provided a more general formula through traction continuity on the kink band boundary:

$$\sigma_1^0 - 2\tau_{13}^0 \tan\beta = \frac{\tau_{13} - \tau_{13}^0 + \sigma_3 \tan\beta}{\phi + \phi_0} \tag{2.5}$$

connecting the applied stresses σ_1^0, τ_{13}^0 the kink band rotation angle, ϕ, and the stresses τ_{13} and σ_3 that develop in the kink band. In the case of zero kink band angle ($\beta = 0$) and a pure compressive stress ($\tau_{13}^0 = 0$), eqn (2.5) reduces to eqn (2.4) with the criterion, $\tau_{13} = k^c$. Fleck (1997) has also analyzed the effects of imperfection size and shape. Jelf and Fleck (1992) found that σ_1^c is linear in k^m, the shear yield stress of the matrix, and suggested that the misalignment angle ϕ_0 in eqn (2.3) is about 3°. Budiansky and Fleck (1993) found that smaller fiber misalignment angles, of the order of 2°, are given by eqn (2.4). Christoffersen and Jensen (1996) and Jensen and Christoffersen (1997) brought the kink band analysis into a standard framework for analyzing localized deformation, and their work regarded kink band formation and shear band formation as two equivalent failure mechanisms. However, in the kink band analysis the fibers are usually assumed to be rigid with respect to longitudinal straining, and have the effect of shielding the matrix from axial compressive stress (Budiansky and Fleck, 1993).

2.3. Kink band angle

Budiansky (1983) provided a micromechanics model for kink band angle β through an approximate computation of the stress for kink band formation for two hypothetical cases of initial short-wave and long-wave imperfections. His expression for long-wave imperfection (similar to the short-wave imperfection case) gives the following result

$$\sigma_1^c = G_{13}^c - E_3^c \tan^2\beta \tag{2.6}$$

where E_3^c is the composite Young's modulus in the transverse direction. Chaudhuri (1991) found a result that is coincidentally identical to eqn (2.6) by accounting for initial fiber misalignment in his microbuckling analysis. Equation (2.6) can predict realistic values for the kink band angle if the compressive strength is known. However, as Chaudhuri (1991) pointed out, eqn (2.6) is in contradiction to the extension of the Budiansky (1983) relationship in an elastic microbuckling analysis, which gives,

$$\sigma_1^c = G_{13}^c + E_3^c \tan^2\beta \tag{2.7}$$

Budiansky (1983) himself has recognized that eqn (2.7) gives $\beta = 0$ as the critical angle for kink band formation. Steif (1990) used a very different approach based on a comparison of the energies of the kinked and unkinked configurations, and he found that the critical stress could approach the minimum as β approaches 45°. But it is observed experimentally that kink bands are inclined typically at $\beta = 20^\circ \sim 30^\circ$ (e.g., Moran et al., 1995; Schultheisz and Waas, 1996). Recently, the kink band angle problem has drawn considerable interest both in analytical and experimental investigations (Kyriakides et al., 1995; Schapery, 1995; Daniel et al., 1996; Vogler and Kyriakides, 1997; Kyriakides and Ruff, 1997; Jensen and Christoffersen, 1997; Christensen and DeTeresa, 1997; Moran and Shih, 1998; Hsu et al., 1998). However, as pointed out by Budiansky et al. (1998), easy recipes for the kink band angle β are not yet available.

3. Microbuckling analysis of perfect composites

As mentioned above, in the elastic microbuckling analyses the two simplest fiber buckling modes commonly assumed have been the extensional mode and the shear mode (Rosen, 1965; Chung and Testa, 1968; Stief, 1987), as shown in Fig. 1(a) and (b), respectively. A representative element of a two-

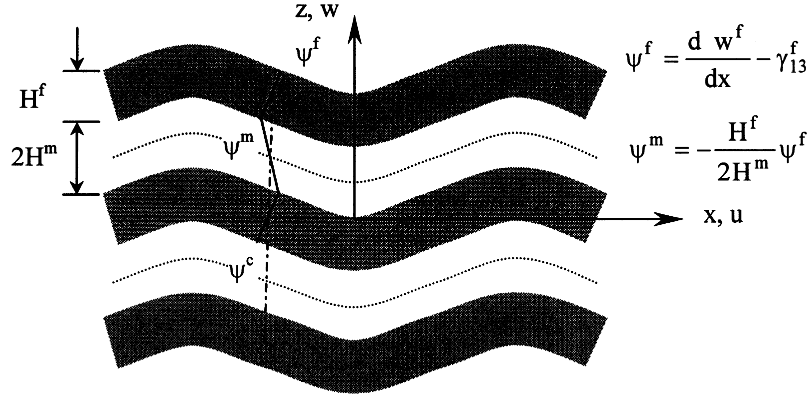

Fig. 2. Shear mode in a generalized Timoshenko beam model.

dimensional model of unit thickness consists of a long fiber embedded in a homogeneous matrix. It is assumed that the deformation is small and the properties of the constituent materials are isotropic and linearly elastic. A possible instability in the matrix material itself is excluded. Further details of the classical microbuckling analysis are given in the Appendix.

Only the shear mode is considered in this paper, as shown in Fig. 2. To account for shear deformation effects in the composite we adopt the Timoshenko shear deformation beam theory for the fiber and treat the matrix as an elastic foundation. The potential energy of the Timoshenko beam with distributed loads is given by,

$$\Pi^{\mathrm{f}} = \frac{D^{\mathrm{f}}}{2}\int_0^L \left(\frac{\mathrm{d}\psi^{\mathrm{f}}}{\mathrm{d}x}\right)^2 \mathrm{d}x + \frac{G^{\mathrm{f}}A^{\mathrm{r}}}{2\alpha}\int_0^L \left(\frac{\mathrm{d}w^{\mathrm{f}}}{\mathrm{d}x} - \psi^{\mathrm{r}}\right)^2 \mathrm{d}x - \frac{P^{\mathrm{f}}}{2}\int_0^L \left(\frac{\mathrm{d}w^{\mathrm{f}}}{\mathrm{d}x}\right)^2 \mathrm{d}x - \int_0^L \left(m^{\mathrm{f}}\psi^{\mathrm{f}} + q^{\mathrm{f}}w^{\mathrm{f}}\right)\mathrm{d}x - M^{\mathrm{f}}\psi^{\mathrm{f}}|_0^L - V^{\mathrm{f}}w^{\mathrm{f}}|_0^L \tag{3.1}$$

where w is the vertical displacement of the fiber neutral axis, D is the bending stiffness about the y-axis, which for a beam is $D = EI$, I being the second moment of the cross-sectional area about the y-axis, and for a plate $D = EI/(1 - \nu_{12}\nu_{21})$, where ν_{12} and ν_{21} are the major and minor Poisson's ratios in the x–y plane, respectively; ψ is the angular rotation of the planar cross section, A is the cross-sectional area which is equal to the height H (thickness equals unity), α is the shear correction factor (in the classical beam theory $\alpha = 1.2$ for a rectangular cross section and $\alpha = 1.11$ for a circular cross section); L is the fiber length, P is the axial compressive force, $M|_0^L$ are end bending moments, $V|_0^L$ are end vertical constraint forces; q is the applied distributed transverse force and m is the distributed bending moment due to the distributed shear stress on the fiber surface. If the distributed loads are not taken into account, the expression will reduce to the classical result (Hu, 1984).

The uniform shear strain of the fiber according to the Timoshenko beam theory is written as

$$\gamma_{13}^{\mathrm{f}} = \frac{\mathrm{d}w^{\mathrm{f}}}{\mathrm{d}x} - \psi^{\mathrm{f}} \tag{3.2}$$

The shear strain field of the matrix is also assumed to be uniform, as shown in Fig. 2. Due to the displacement continuity at the interface between the fiber and the matrix, the angular rotation of the matrix corresponding to the angular rotation of the fiber planar cross section is given by,

$$\psi^{\mathrm{m}} = -\frac{\partial u^{\mathrm{m}}}{\partial z} = -\frac{H^{\mathrm{f}}}{2H^{\mathrm{m}}}\psi^{\mathrm{f}} = -\frac{v^{\mathrm{f}}}{1-v^{\mathrm{f}}}\psi^{\mathrm{f}} \tag{3.3}$$

where the fiber volume fraction is given by,

$$v^{\mathrm{f}} = \frac{H^{\mathrm{f}}}{H^{\mathrm{f}} + 2H^{\mathrm{m}}} \tag{3.4}$$

The total matrix shear strain is given by,

$$\gamma_{13}^{\mathrm{m}} = \frac{\partial w^{\mathrm{m}}}{\partial x} + \frac{\partial u^{\mathrm{m}}}{\partial z} = \frac{\mathrm{d}w^{\mathrm{f}}}{\mathrm{d}x} + \frac{v^{\mathrm{f}}\psi^{\mathrm{f}}}{1-v^{\mathrm{f}}} = \frac{\mathrm{d}w^{\mathrm{f}}}{\mathrm{d}x} - \psi^{\mathrm{m}} \tag{3.5}$$

The uniform shear stress in the fiber is

$$\tau_{13}^{\mathrm{f}} = G^{\mathrm{f}}\gamma_{13}^{\mathrm{f}} = G^{\mathrm{f}}\left(\frac{\mathrm{d}w^{\mathrm{f}}}{\mathrm{d}x} - \psi^{\mathrm{f}}\right) \tag{3.6}$$

i.e., $\alpha = 1$, and the shear stress in the matrix is also uniform and is given by,

$$\tau_{13}^{\mathrm{m}} = G^{\mathrm{m}}\gamma_{13}^{\mathrm{m}} = \frac{G^{\mathrm{m}}}{1-v^{\mathrm{f}}}\frac{\mathrm{d}w^{\mathrm{f}}}{\mathrm{d}x} - \frac{v^{\mathrm{f}}G^{\mathrm{m}}}{1-\upsilon^{\mathrm{f}}}\left(\frac{\mathrm{d}w^{\mathrm{f}}}{\mathrm{d}x} - \psi^{\mathrm{f}}\right) \tag{3.7}$$

Since traction is continuous on the fiber/matrix interface, $\tau_{13}^{\mathrm{f}} = \tau_{13}^{\mathrm{m}}$, and we have,

$$\tau_{13}^{\mathrm{f}} = \tau_{13}^{\mathrm{m}} = \frac{G^{\mathrm{f}}G^{\mathrm{m}}}{(1-v^{\mathrm{f}})G^{\mathrm{f}} + v^{\mathrm{f}}G^{\mathrm{m}}}\frac{\mathrm{d}w^{\mathrm{f}}}{\mathrm{d}x} = G_{13}^{\mathrm{c}}\frac{\mathrm{d}w^{\mathrm{f}}}{\mathrm{d}x} \tag{3.8}$$

and

$$\psi^{\mathrm{f}} = \frac{(1-v^{\mathrm{f}})(G^{\mathrm{f}} - G^{\mathrm{m}})}{(1-v^{\mathrm{f}})G^{\mathrm{f}} + v^{\mathrm{f}}G^{\mathrm{m}}}\frac{\mathrm{d}w^{\mathrm{f}}}{\mathrm{d}x} \tag{3.9}$$

Here, the effective shear modulus is defined in accordance with the 'inverse rule of mixtures' as

$$G_{13}^{\mathrm{c}} = \left(\frac{v^{\mathrm{f}}}{G^{\mathrm{f}}} + \frac{1-v^{\mathrm{f}}}{G^{\mathrm{m}}}\right)^{-1} \tag{3.10}$$

The above result uses the same assumption as in the slab model. The assumption of the uniform matrix shear deformation in eqn (3.5) is a strong constraint in this analysis and will be discussed in Section 7. The shear stress distribution in the classical Timoshenko beam is not used here because the periodic matrix–fiber–matrix structure is more like an infinite thickness laminate. According to the classical laminate theory, the shear stress is uniformly distributed in each layer.

Equation (3.8) is a very important result of the shear stress–strain relationship of the composite in the microbuckling analysis. The shear strain and stress of the composite can then be defined as

$$\tau_{13}^{\mathrm{c}} = G_{13}^{\mathrm{c}}\frac{\mathrm{d}w^{\mathrm{f}}}{\mathrm{d}x} = G_{13}^{\mathrm{c}}\gamma_{13}^{\mathrm{c}}, \quad \text{and} \quad \gamma_{13}^{\mathrm{c}} = \frac{\mathrm{d}w^{\mathrm{f}}}{\mathrm{d}x} \tag{3.11}$$

respectively. From these definitions, shear strains are different in composite, fibers, and matrix, and their relations are

$$\frac{\mathrm{d}w^{\mathrm{f}}}{\mathrm{d}x} - \psi^{\mathrm{f}} = \gamma_{13}^{\mathrm{f}} < \gamma_{13}^{\mathrm{c}} = \frac{\mathrm{d}w^{\mathrm{f}}}{\mathrm{d}x} < \gamma_{13}^{\mathrm{m}} = \frac{\mathrm{d}w^{\mathrm{f}}}{\mathrm{d}x} + \frac{v^{\mathrm{f}}\psi^{\mathrm{f}}}{1 - v^{\mathrm{f}}} \tag{3.12}$$

But shear stresses are the same, i.e.,

$$\tau_{13}^{\mathrm{c}} = \tau_{13}^{\mathrm{f}} = \tau_{13}^{\mathrm{m}} \tag{3.13}$$

In fact, the shear strain of the composite can be defined alternatively by

$$\gamma_{13}^{\mathrm{c}} = v^{\mathrm{f}}\gamma_{13}^{\mathrm{f}} + (1 - v^{\mathrm{f}})\gamma_{13}^{\mathrm{m}} = \frac{\mathrm{d}w^{\mathrm{f}}}{\mathrm{d}x} \tag{3.14}$$

using eqns (3.2) and (3.5). This is the ‘rule of mixture’ of shear strains in the fiber and the matrix. If the representative element of the composite is treated as the Timoshenko beam, we will have

$$\frac{\mathrm{d}w^{\mathrm{c}}}{\mathrm{d}x} = \frac{\mathrm{d}w^{\mathrm{f}}}{\mathrm{d}x}, \quad \text{and} \quad \psi^{\mathrm{c}} = v^{\mathrm{f}}\psi^{\mathrm{f}} + (1 - v^{\mathrm{f}})\psi^{\mathrm{m}} = 0 \tag{3.15}$$

using eqn (3.3). The second expression also means that no global bending is involved in the representative element even though each single fiber is in a flexural buckling state as shown in Fig. 2, and, therefore, the analysis is only applicable for pure microbuckling.

Since there is not lateral extension or compression in the matrix, the normal distributed load can be assumed as

$$q^{\mathrm{f}} = 0 \tag{3.16}$$

The distributed moment due to surface shear stress is

$$m^{\mathrm{f}} = -H^{\mathrm{f}}\tau_{13}^{\mathrm{f}} \tag{3.17}$$

However, if we add shear stress acting in the matrix, but do not account for the matrix bending stiffness, i.e., $D^{\mathrm{m}} = 0$, the moment in the representative element of the composite becomes

$$m^{\mathrm{c}} = -H^{\mathrm{f}}\tau_{13}^{\mathrm{f}} - 2H^{\mathrm{m}}\tau_{13}^{\mathrm{m}} = -\left(H^{\mathrm{f}} + 2H^{\mathrm{m}}\right)\tau_{13}^{\mathrm{m}} \tag{3.18}$$

Since both the top face and bottom face of the representative element are in an antisymmetric position of the periodic matrix–fiber–matrix structure, the distributed moment contributes no work during the buckling perturbation because $\psi^{\mathrm{c}} = 0$, as shown by eqn (3.15).

The total potential energy of the representative element is

$$\begin{aligned}
\Pi = \Pi^{\mathrm{f}} + \Pi^{\mathrm{m}} &= \frac{D^{\mathrm{f}}}{2}\int_0^L \left(\frac{\mathrm{d}\psi^{\mathrm{f}}}{\mathrm{d}x}\right)^2 \mathrm{d}x + \left(\frac{H^{\mathrm{f}}}{2G^{\mathrm{f}}} + \frac{H^{\mathrm{m}}}{G^{\mathrm{m}}}\right)\int_0^L \left(G_{13}^{\mathrm{c}}\frac{\mathrm{d}w^{\mathrm{f}}}{\mathrm{d}x}\right)^2 \mathrm{d}x \\
&\quad - \frac{P^{\mathrm{f}}}{2}\int_0^L \left(\frac{\mathrm{d}w^{\mathrm{f}}}{\mathrm{d}x}\right)^2 \mathrm{d}x - \int_0^L m^{\mathrm{c}}\psi^{\mathrm{c}}\,\mathrm{d}x - M^{\mathrm{f}}\psi^{\mathrm{f}}|_0^L - V^{\mathrm{f}}w^{\mathrm{f}}|_0^L \\
&= \frac{D^{\mathrm{f}}}{2}\int_0^L \left[\frac{(1 - v^{\mathrm{f}})(G^{\mathrm{f}} - G^{\mathrm{m}})}{(1 - v^{\mathrm{f}})G^{\mathrm{f}} + v^{\mathrm{f}}G^{\mathrm{m}}}\frac{\mathrm{d}^2 w^{\mathrm{f}}}{\mathrm{d}x}\right]^2 \mathrm{d}x + \frac{H^{\mathrm{f}} + 2H^{\mathrm{m}}}{2}\int_0^L G_{13}^{\mathrm{c}}\left(\frac{\mathrm{d}w^{\mathrm{f}}}{\mathrm{d}x}\right)^2 \mathrm{d}x \\
&\quad - \frac{P^{\mathrm{f}}}{2}\int_0^L \left(\frac{\mathrm{d}w^{\mathrm{f}}}{\mathrm{d}x}\right)^2 \mathrm{d}x - M^{\mathrm{f}}\frac{(1 - v^{\mathrm{f}})(G^{\mathrm{f}} - G^{\mathrm{m}})}{(1 - v^{\mathrm{f}})G^{\mathrm{f}} + v^{\mathrm{f}}G^{\mathrm{m}}}\left.\frac{\mathrm{d}w^{\mathrm{f}}}{\mathrm{d}x}\right|_0^L - V^{\mathrm{f}}w^{\mathrm{f}}\Big|_0^L
\end{aligned} \tag{3.19}$$

where eqns (3.8) and (3.9) have been applied. According to the principle of minimum potential energy the stationarity condition $\delta\Pi = 0$ yields

$$\left[\frac{(1-v^{\mathrm{f}})(G^{\mathrm{f}}-G^{\mathrm{m}})}{(1-v^{\mathrm{f}})G^{\mathrm{f}}+v^{\mathrm{f}}G^{\mathrm{m}}}\right]^2 D^{\mathrm{f}}\frac{\mathrm{d}^4w^{\mathrm{f}}}{\mathrm{d}x^4}+\left(P^{\mathrm{f}}-\frac{H^{\mathrm{f}}}{v^{\mathrm{f}}}G_{13}^{\mathrm{c}}\right)\frac{\mathrm{d}^2w^{\mathrm{f}}}{\mathrm{d}x^2}=0 \tag{3.20}$$

$$\left[\frac{(1-v^{\mathrm{f}})(G^{\mathrm{f}}-G^{\mathrm{m}})}{(1-v^{\mathrm{f}})G^{\mathrm{f}}+v^{\mathrm{f}}G^{\mathrm{m}}}D^{\mathrm{f}}\frac{\mathrm{d}^2w^{\mathrm{f}}}{\mathrm{d}x^2}-M^{\mathrm{f}}\right]\delta\frac{\mathrm{d}w^{\mathrm{f}}}{\mathrm{d}x}\bigg|_0^L=0 \tag{3.21}$$

$$\left\{\left[\frac{(1-v^{\mathrm{f}})(G^{\mathrm{f}}-G^{\mathrm{m}})}{(1-v^{\mathrm{f}})G^{\mathrm{f}}+v^{\mathrm{f}}G^{\mathrm{m}}}\right]^2 D^{\mathrm{f}}\frac{\mathrm{d}^3w^{\mathrm{f}}}{\mathrm{d}x^3}+\left(P^{\mathrm{f}}-\frac{H^{\mathrm{f}}}{v^{\mathrm{f}}}G_{13}^{\mathrm{c}}\right)\frac{\mathrm{d}w^{\mathrm{f}}}{\mathrm{d}x}+V^{\mathrm{f}}\right\}\delta w^{\mathrm{f}}|_0^L=0 \tag{3.22}$$

The last two equations represent the boundary conditions. The first is the governing buckling equation comparable to the Euler beam buckling equation.

The critical buckling load is

$$P^{\mathrm{f}}=\frac{H^{\mathrm{f}}}{v^{\mathrm{f}}}G_{13}^{\mathrm{c}}+\left[\frac{(1-v^{\mathrm{f}})(G^{\mathrm{f}}-G^{\mathrm{m}})}{(1-v^{\mathrm{f}})G^{\mathrm{f}}+v^{\mathrm{f}}G^{\mathrm{m}}}\right]^2\frac{\pi^2D^{\mathrm{f}}}{\left(\hat{L}L\right)^2} \tag{3.23}$$

where $\hat{L}$ is the normalized effective length of the Euler beam. For example, $\hat{L}=1$ for a simply supported boundary condition, $\hat{L}=0.5$ for a fixed–fixed boundary condition, etc. If the fiber length L is large enough, the second term in eqn (3.23) is negligible and all boundary conditions will give the same buckling load. The well-known general Rosen expression is then obtained as

$$\sigma_1^{\mathrm{c}}=v^{\mathrm{f}}\frac{P^{\mathrm{f}}}{H^{\mathrm{f}}}=G_{13}^{\mathrm{c}} \tag{3.24}$$

If G^{f} is large or v^{f} is small, eqn (3.24) will reduce to Rosen's eqn (2.1) according to eqn (3.10). Experiments (Greszczuk, 1974; Jelf and Fleck, 1992; Fleck, 1997) have confirmed that eqn (3.24) is accurate when the matrix behaves in a linear elastic manner.

Based on a new generalized Timoshenko beam model above, we have now proven the general Rosen formula and have obtained very important relationships given in eqns (3.8) and (3.11). Several papers (Foye, 1966; Kulkarni et al., 1975; Yeh and Teply, 1988; Chaudhuri, 1991, etc.) have also shown that G_{13}^{c} in eqn (3.24) is the same expression as in eqn (3.10). But in these works the shear deformation has not been introduced through the Timoshenko beam theory and the shear stress–strain relationship in eqn (3.8) and the definition of the shear strain in eqn (3.11) have not been applied. We will use eqns (3.8) and (3.11) in our misalignment microbuckling analysis in the following section.

4. Microbuckling analysis for misalignment defects

An initial fiber transverse misalignment w_0^{f} with arbitrary shape is assumed to be very small, and will have no major effect on what we have developed above. The total potential energy of the representative element is modified as

$$\Pi = \frac{D^{\mathrm{f}}}{2}\int_0^L \left[\frac{(1-v^{\mathrm{f}})(G^{\mathrm{f}}-G^{\mathrm{m}})}{(1-v^{\mathrm{f}})G^{\mathrm{f}}+v^{\mathrm{f}}G^{\mathrm{m}}}\frac{\mathrm{d}^2 w^{\mathrm{f}}}{\mathrm{d}x^2}\right]^2 \mathrm{d}x + \frac{H^{\mathrm{f}}+2H^{\mathrm{m}}}{2}\int_0^L G_{13}^{\mathrm{c}}\left(\frac{\mathrm{d}w^{\mathrm{f}}}{\mathrm{d}x}\right)^2 \mathrm{d}x$$
$$-\frac{P^{\mathrm{f}}}{2}\int_0^L\left[\left(\frac{\mathrm{d}w^{\mathrm{f}}}{\mathrm{d}x}\right)^2 + 2\frac{\mathrm{d}w_0^{\mathrm{f}}}{\mathrm{d}x}\frac{\mathrm{d}w^{\mathrm{f}}}{\mathrm{d}x}\right]\mathrm{d}x - M^{\mathrm{f}}\frac{(1-v^{\mathrm{f}})(G^{\mathrm{f}}-G^{\mathrm{m}})}{(1-v^{\mathrm{f}})G^{\mathrm{f}}+v^{\mathrm{f}}G^{\mathrm{m}}}\frac{\mathrm{d}w^{\mathrm{f}}}{\mathrm{d}x}\bigg|_0^L - V^{\mathrm{f}}w^{\mathrm{f}}\bigg|_0^L \tag{4.1}$$

where eqns (3.8) and (3.9) have been applied. The stationarity condition $\delta\Pi = 0$ now becomes

$$\left[\frac{(1-v^{\mathrm{f}})(G^{\mathrm{f}}-G^{\mathrm{m}})}{(1-v^{\mathrm{f}})G^{\mathrm{f}}+v^{\mathrm{f}}G^{\mathrm{m}}}\right]^2 D^{\mathrm{f}}\frac{\mathrm{d}^4 w^{\mathrm{f}}}{\mathrm{d}x^4} + \left(P^{\mathrm{f}} - \frac{H^{\mathrm{f}}}{v^{\mathrm{f}}}G_{13}^{\mathrm{c}}\right)\frac{\mathrm{d}^2 w^{\mathrm{f}}}{\mathrm{d}x^2} + P^{\mathrm{f}}\frac{\mathrm{d}^2 w_0^{\mathrm{f}}}{\mathrm{d}x^2} = 0 \tag{4.2}$$

$$\left[\frac{(1-v^{\mathrm{f}})(G^{\mathrm{f}}-G^{\mathrm{m}})}{(1-v^{\mathrm{f}})G^{\mathrm{f}}+v^{\mathrm{f}}G^{\mathrm{m}}}D^{\mathrm{f}}\frac{\mathrm{d}^2 w^{\mathrm{f}}}{\mathrm{d}x^2} - M^{\mathrm{f}}\right]\delta\frac{\mathrm{d}w^{\mathrm{f}}}{\mathrm{d}x}\bigg|_0^L = 0 \tag{4.3}$$

$$\left\{\left[\frac{(1-v^{\mathrm{f}})(G^{\mathrm{f}}-G^{\mathrm{m}})}{(1-v^{\mathrm{f}})G^{\mathrm{f}}+v^{\mathrm{f}}G^{\mathrm{m}}}\right]^2 D^{\mathrm{f}}\frac{\mathrm{d}^3 w^{\mathrm{f}}}{\mathrm{d}x^3} + \left(P^{\mathrm{f}} - \frac{H^{\mathrm{f}}}{v^{\mathrm{f}}}G_{13}^{\mathrm{c}}\right)\frac{\mathrm{d}w^{\mathrm{f}}}{\mathrm{d}x} + P^{\mathrm{f}}\frac{\mathrm{d}w_0^{\mathrm{f}}}{\mathrm{d}x} + V^{\mathrm{f}}\right\}\delta w^{\mathrm{f}}\bigg|_0^L = 0 \tag{4.4}$$

The initial misalignment of the fiber may be assumed to be sinusoidal wave, as

$$w_0^{\mathrm{f}} = a_0 \sin\frac{n\pi x}{L} \tag{4.5}$$

where a_0 is the maximum initial transverse displacement and $n+1$ is the node number of the sinusoidal waveform. For the fiber pinned at both ends, a sinusoidal solution satisfies boundary conditions and is assumed as

$$w^{\mathrm{f}} = a_n \sin\frac{n\pi x}{L} \tag{4.6}$$

where a_n is the maximum increment of transverse displacement corresponding to the mode shape. The fiber buckling load is

$$P^{\mathrm{f}} = \frac{a_n}{a_n + a_0}\left[\frac{H^{\mathrm{f}}}{v^{\mathrm{f}}}G_{13}^{\mathrm{c}} + \left[\frac{(1-v^{\mathrm{f}})(G^{\mathrm{f}}-G^{\mathrm{m}})}{(1-v^{\mathrm{f}})G^{\mathrm{f}}+v^{\mathrm{f}}G^{\mathrm{m}}}\right]^2 D^{\mathrm{f}}\left(\frac{n\pi}{L}\right)^2\right] \tag{4.7}$$

If the second term is negligible, e.g., for large L, a simple relation between compressive stress and transverse displacement is obtained as [similar to (A.30)]

$$\sigma_1^{\mathrm{c}} = \frac{E_1^{\mathrm{d}}\sigma_1^{\mathrm{f}}}{E} \cong \frac{a_n}{a_n + a_0}G_{13}^{\mathrm{c}} \tag{4.8}$$

Comparing eqn (4.8) with $\sigma_1^{\mathrm{c}} = G_{13}^{\mathrm{c}}$ in eqn (3.24), there is a knockdown factor of less than 1. However, a buckling stress can be given by eqn (4.8) only when the amplitude a_n is very large, i.e., $a_n \gg a_0$, and it will then be $\sigma_1^{\mathrm{c}} = G_{13}^{\mathrm{c}}$. If $\sigma_1^{\mathrm{c}} \ll G_{13}^{\mathrm{c}}$, the solution of eqn (4.2) will never result in buckling.

An additional failure criterion has to be applied to (4.8) if the matrix properties are involved. According to eqn (3.8), the maximum shear stress in matrix can be written as

$$\tau_{13}^{\mathrm{m}}\big|_{\max} = G_{13}^{\mathrm{c}}\left|\frac{\mathrm{d}w^{\mathrm{f}}}{\mathrm{d}x}\right|_{\max} = a_n\frac{n\pi}{L}G_{13}^{\mathrm{c}} \tag{4.9}$$

Therefore, eqn (4.8) can be rewritten as a failure expression as

$$\sigma_1^{\mathrm{c}} = \frac{\tau_f^{\mathrm{c}}}{\gamma_f^{\mathrm{c}} + \phi_0} = \frac{G_{13}^{\mathrm{c}}}{1 + \phi_0/\gamma_f^{\mathrm{c}}} \tag{4.10}$$

where

$$\tau_{\mathrm{f}}^{\mathrm{c}} = \tau_{13}^{\mathrm{m}}|_{\max} = G_{13}^{\mathrm{c}}\gamma_{\mathrm{f}}^{\mathrm{c}}; \quad \gamma_{\mathrm{f}}^{\mathrm{c}} = a_n\frac{n\pi}{L}; \quad \phi_0 = a_0\frac{n\pi}{L} \tag{4.11}$$

Note that ϕ_0 is defined as the maximum angle of the initial fiber misalignment.

Composite failure can be triggered by different mechanisms. Three models have been proposed as: (1) matrix yielding in a perfectly plastic matrix (Argon, 1972; Budiansky, 1983); (2) fiber–matrix interface debonding (Lanir and Fung, 1972); (3) matrix microcracks (Schapery, 1995). Note, for example, that letting $\tau_{\mathrm{f}}^{\mathrm{c}} = k^{\mathrm{c}}$ in eqn (4.10) will give an expression identical to eqn (2.4) (Budiansky, 1983) for a perfectly plastic composite. A general relation is obtained as

$$\sigma_1^{\mathrm{c}} = \frac{k^{\mathrm{c}}}{\gamma_{\mathrm{y}}^{\mathrm{c}} + \phi_0} = \frac{G_{13}^{\mathrm{c}}}{1 + \phi_0/\gamma_{\mathrm{y}}^{\mathrm{c}}} < \frac{G_{13}^{\mathrm{c}}}{1 + \phi_0/\gamma_{\mathrm{y}}^{\mathrm{m}}} \tag{4.12}$$

since $\gamma_{\mathrm{y}}^{\mathrm{c}} = k^{\mathrm{c}}/G_{13}^{\mathrm{c}} < \gamma_{\mathrm{y}}^{\mathrm{m}}$ from eqn (3.12).

Obviously, matrix deformation during buckling perturbation needs to be considered to lead to a more rigorous prediction (Chung and Testa, 1968; Stief, 1987). One way to modify the composite buckling analysis is to add the matrix bending stiffness. This will result in a global beam buckling analysis, i.e., a macrobuckling model, which will be discussed in the next section.

5. 'Shear hinge' analysis

Once a kink band is triggered, the kink band section can be considered to play a role similar to an elastoplastic hinge in the plastic buckling analysis of beams. We may call the kink band section a 'shear hinge'. The reason is that the buckling state is in a 'transverse shear induced buckling' mode instead of a flexural buckling mode, provided that shear stress reaches a critical value. Before we discuss the 'shear hinge', a review of the method of split rigidities will be appropriate.

The method of split rigidities was proposed by Bijlaard (1951) for estimating the critical buckling loads of sandwich panels. The method has lately been extended to static and vibration problems by Hu (1984). The method of split rigidities is a very intuitive one for the Timoshenko beam analysis. There are two independent variables: w and ψ, where w is the lateral displacement of the beam neutral line, and ψ is the angular rotation of the beam planar cross section. If the shear stiffness is assumed to be infinitely large, the buckling load is reduced to the Euler critical load for the corresponding boundary conditions as

$$P_{\mathrm{e}} = \frac{\pi^2 D^{\mathrm{c}}}{\left(\hat{L}L\right)^2} \tag{5.1}$$

If the bending stiffness is assumed to be infinitely large, the shear buckling load is simply (Hu, 1984)

$$P_{\mathrm{s}} = \frac{G_{13}^{\mathrm{c}} A}{\alpha} \tag{5.2}$$

The method of split rigidities assumes that the global buckling load can be given by

$$\frac{1}{P} = \frac{1}{P_e} + \frac{1}{P_s} \tag{5.3}$$

Equation (5.3) is an exact solution of the buckling load in the Timoshenko beam theory. It is to be noted that, as shown by Hu (1984) by an energy method, a solution obtained by the split rigidity method forms an upper bound to the exact solution of the buckling load. However, when the Timoshenko beam theory is used, eqn (5.3) becomes the exact solution.

Alternatively, the Euler critical stress is defined as

$$\sigma_e = \frac{P_e}{A} \tag{5.4}$$

and the shear critical stress is defined as

$$\sigma_s = \frac{P_s}{A} \tag{5.5}$$

An expression for the critical stress σ can now be written as

$$\frac{1}{\sigma} = \frac{1}{\sigma_e} + \frac{1}{\sigma_s} \tag{5.6}$$

If the Euler critical stress is much larger than the critical shear stress, then

$$\sigma \cong \sigma_s = \frac{G_{13}^c}{\alpha} \tag{5.7}$$

As shown by Chou and Kelly (1980), eqn (5.7) is equivalent to Rosen's microbuckling shear mode when the shear stress distribution is accounted for. We propose that the method of split rigidities can be naturally extended to the microbuckling analysis.

By virtue of the method of split rigidities, only the shear buckling mode needs to be discussed here if the total length of the beam, L, is relatively short. A special shear hinge is designed to simulate the kink band mechanism in Fig. 3. It is assumed that the bending stiffness of the beam is infinitely large and therefore only the shear deformation is allowable in the beam. The instability criterion can be obtained

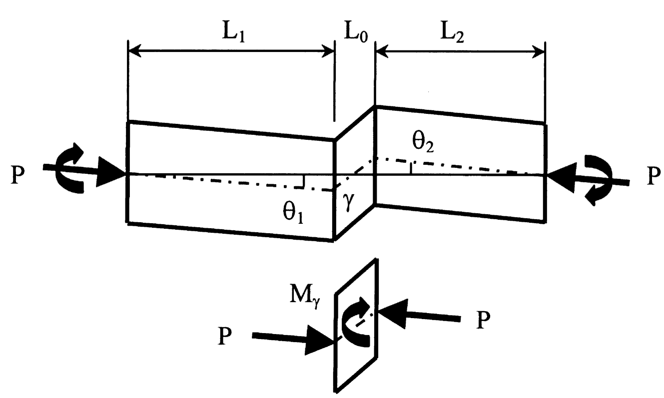

Fig. 3. 'Shear hinge' simulating a kink band in a representative element with a misaligned compressive load.

for a small shear perturbance of the inclination in Fig. 3. For a force balance in the vertical direction,

$$P\theta_1 = P\theta_2, \quad \text{or } \theta = \theta_1 = \theta_2 \tag{5.8}$$

for small θ_1 and θ_2. The rotation of the neutral line in the section L_0, i.e., the shear strain in the kink band, is defined as

$$\gamma = \frac{L_1\theta_1 + L_2\theta_2}{L_0} = \frac{L - L_0}{L_0}\theta \tag{5.9}$$

If the beam length L is much larger than the kink band section L_0, the shear strain, θ, in the sections L_1 and L_2 must be much smaller than γ in the kink band. The kink band section may then be viewed as a 'shear hinge' (similar to 'plastic hinge' in bending of beams).

Since we assume the bending stiffness to be infinitely large, any bending effect can be excluded from the analysis. A torque moment due to the shear perturbance γ in the 'shear hinge' section L_0 is found as

$$M_\gamma = L_0 A \tau(\gamma) \tag{5.10}$$

as the 'shear hinge' acts as a rotary spring. If the shear stress distribution is accounted for, the moment is modified as

$$M_\gamma = L_0 A \frac{\tau(\gamma)}{\alpha} \tag{5.11}$$

where the shear stress $\tau(\gamma)$ is considered as an average value in the beam theory.

In a perfectly aligned fiber composite and load system, a state of static equilibrium of the 'shear hinge' for a given shear perturbation only gives

$$M_\gamma = L_0 P \sin\gamma \tag{5.12}$$

From eqns (5.10) and (5.12) the critical shear buckling stress for elastic case is found to be

$$\sigma = \frac{P}{A} = \frac{\tau}{\gamma} = G_{13}^{c} \tag{5.13}$$

where $\sin\gamma \cong \gamma$ is used. If eqn (5.11) instead of (5.10) is used, the expression will be the same as eqn (5.7). Thus, the Rosen formula is recovered.

For a beam with a small initial misalignment ϕ_0 and a load system with a small misalignment ϕ_1, the equilibrium state gives

$$M_\gamma = L_0 P \sin\left(\gamma + \phi_0 + \phi_1\right) \tag{5.14}$$

This buckled state in the 'shear hinge' is then represented by

$$\sigma = \frac{\tau(\gamma)}{\sin\left(\gamma + \phi_0 + \phi_1\right)} \tag{5.15}$$

The expression is similar to that by a simple model consisting of a vertical rigid rod suffering some initial deviation and having a rotation-constrained spring, for example, in the comprehensive overview by Budiansky (1974). This kind of buckling has been called snap buckling, and the critical stress is very sensitive to imperfections ϕ_0 and ϕ_1. Similar to the previous section, the critical stress may be written as

$$\sigma = \frac{\tau_f^c}{\gamma_f^c + \phi_0 + \phi_1} \tag{5.16}$$

for small angles. This expression looks similar to eqn (4.10). However, the interpretation is, somewhat, different. Here ϕ_0 is the maximum inclination of the beam, and ϕ_1 is the misinclination in the loading system. Now we have extended the Argon–Budiansky kinking stress expression including misalignments of both fibers and loading system. Wisnom (1990) seems to be the first to discuss the effect of a uniform misalignment angle between the fibers and loading axis, and he deduced eqn (2.4) by regarding a unidirectional layer of straight fibers aligned at an angle to the loading axis.

6. Kink band angle

It is interesting to compare the results above to the kinking failure mechanism of a perfectly plastic composite as discussed by Argon (1972). His argument is that if the interlaminar shear strength criterion, $k = \sigma^c \phi_0$, is reached, an additional rotation ϕ will develop and ϕ_0 is then interpreted as the initial misalignment of fibers. However, as we will discuss in the next section, the lamellae sliding and rotating depend on the matrix yielding condition which is dependent on both the axial normal compressive stress and the shear stress due to the initial misalignment of fibers. In an extreme case, assuming perfectly straight fibers, a simple relation for homogeneous matrix materials from the Tresca yield criterion is

$$\sigma_y^m = \frac{2k^m}{\sin(2\omega)} \tag{6.1}$$

where k^m is the shear yield stress of the matrix and ω is the slip line angle. Therefore, σ_y^m achieves a minimum value if ω is 45°. There is no reason to require that ω has the same value as that of the initial misalignment of fibers. In fact, as mentioned in the Introduction section, the axial compressive strain at the point of kink band formation is about 1%, which is of the same order of magnitude as a typical shear yield strain of a polymetric matrix. Furthermore, for a transversely isotropic material loaded normal to the isotropic plane, the planes of maximum shear stress and strain coincide and lie at 45° to the loading axis. It has been argued that it might be expected that the kink band in unidirectional composites would lie along a plane at $\beta = 45°$ since the kink bands resemble shear bands and are therefore associated with large shear deformations (Schultheisz and Waas, 1996). However, experiments have shown that this argument generally does not hold. If kinking is a consequence of purely elastic microbuckling, one would expect the kink band boundary to lie in the plane of the highest bending stress in the fibers, i.e., $\beta = 0$, as in Fig. 2. This is generally not true either. We propose a new theory for the kink band angle in the following.

If the matrix yields, the fiber buckling instability will be induced by a transverse perturbation, as we have discussed above. However, a localized matrix yielding does not necessarily mean composite failure because fibers may stop matrix sliding. Obviously, if matrix sliding induces instability in the neighboring fibers, this instability effect must propagate through the whole cross section of the strip, as shown in Fig. 4, and then a slight misalignment can trigger kink band formation. Otherwise, the slip system will not evolve. From this point of view, a formula for kink band angle can easily be derived. In Fig. 4 the matrix is assumed to slide at the angle ω, and the fiber is in flexural buckling. We also assume that the elastic strain of the matrix is neglected, and the fiber is transversely inextensible and shear stiff. If only the initial kink state is considered for, i.e., $\phi = 0$, the average angle of the slip system is written as

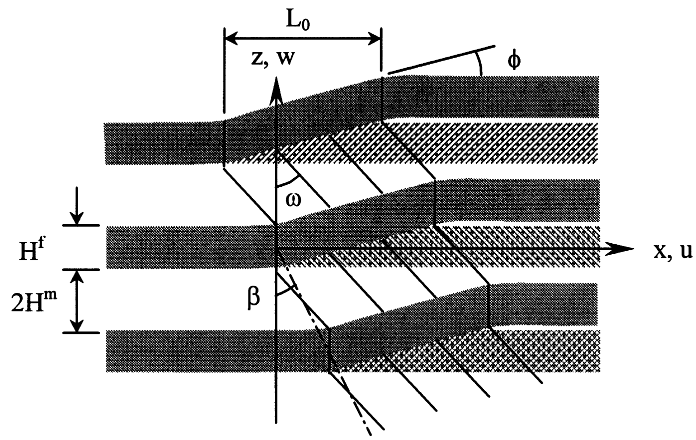

Fig. 4. A model of kink band caused by matrix sliding and fiber buckling.

$$\tan \beta = \frac{2H^{\mathrm{m}}}{H^{\mathrm{f}} + 2H^{\mathrm{m}}} \tan \omega = (1 - v^{\mathrm{f}}) \tan \omega \tag{6.2}$$

Our hypothesis is that the kink band angle, β, is governed by the onset of the kinking state, therefore, eqn (6.2) does not involve any post-kink process. For a composite comprising perfectly straight fibers and a plastic matrix, $\omega = 45^{\circ}$, and the kink band angle is simply

$$\beta = \arctan (1 - v^{\mathrm{f}}) = \arctan (v^{\mathrm{m}}) \tag{6.3}$$

If v^{f} is small, β will be close to 45°. In polymer matrix composites with very low fiber volume fraction, matrix yielding and fracture do occur in a band oriented at about 45° (Fleck, 1997). This failure mechanism is called shear banding, and is essentially equivalent to kink band failure (Christoffersen and Jensen, 1996). In most continuous fiber composites matrix volume fraction lies between 0.4 and 0.6. Estimated angles from eqn (6.3) thus range from 22–31°, and the prediction is reasonably good for most experimental observations (Moran et al., 1995; Schultheisz and Waas, 1996). In the cases of fiber misalignment and notch stress concentration, there will be an additional transverse shear stress in the prebuckling state. Or, if the fiber elastic microbuckling occurs first, additional transverse shear stress will be induced before kink band formation. In these cases $\omega < 45^{\circ}$ and eqn (6.3) will generally give an upper bound to the kink band angle.

Direct experimental evidence to support this analysis comes from compression tests on the composite which has 60% volume fraction of IM7 carbon fibers and a relatively ductile PEEK matrix (Moran et al., 1995). These authors found distinctly different deformation in various stages of the kinking process. In the incipient kinking stage kink band growth is notch sensitive where inelastic behavior is characterized by plastic flow of the matrix in a small region ahead of the specimen notch, and the kink band angle, β, lies between 10 and 15°. However, in the applied peak stress stage the narrow band advances across the rest of the specimen and the dominant kink band is driven by the remote stresses. In this stage the band angle is significantly steeper than that in the incipient kinking stage, and β was measured to be about 22° as predicted accurately by eqn (6.3). Thereafter, the kink band spreads laterally into the specimen by band width broadening and the kink band angle remains unchanged.

We shall make a few further remarks about the new analysis presented above. Equation (6.2) is a simple geometrical relation for the onset of a kink band formation, and no properties of the composite constituents except fiber volume fraction are involved. Fiber bending break in experiments is a result of the fiber post-bucking behavior, and should not be a relevant issue to kink band angles. Shear plastic deformation of the matrix is a requirement only for the kink band initiation, and therefore assumption of a perfectly plastic composite is not necessary. This mechanism also implies that a brittle matrix may not induce a kink band, and it may explain why little experimental evidence is available for kinking mechanism in ceramic matrix composites. In eqn (2.6) by Budiansky (1983), $\sigma_1^c = G_{13}^c - E_3^c \tan^2 \beta$ the kink band angle is related to the axial compressive stress in the composite. On the other hand, this equation could be considered as a modification to $\sigma_1^c = G_{13}^c$ in elastic microbuckling, if one finds a way to determinate β independently such as in eqn (6.2).

7. Discussion

As we have shown in Sections 3–5, both the Rosen formula and the Argon–Budiansky formula can be developed by a microbuckling model and the method of split rigidities. In the generalized Timoshenko beam theory, the shear strains in the matrix and fiber are assumed to be uniform. This uniformity assumption leads to the ‘inverse rule of mixtures’ of the shear modulus [eqn (3.10)] which can be proven to be the socalled Reuss lower bound of the effective shear modulus by the theorem of minimum complementary energy (e.g., Parton and Kudryavtsev, 1993). This means that the generalized Timoshenko beam theory gives the first-order approximation of the exact solution. According to higher order models (Chung and Testa, 1968; Niu and Talreja, 1998), the shear strain uniformity is a reasonable assumption in the shear mode buckling for practical fiber reinforced composites. It is noted that three shear strains have been defined separately for composite, fibers, and matrix in the macrobuckling model [eqn (3.12)] besides smearing out fibers and matrix in the microbuckling model.

In the microbuckling model, eqn (4.10) is based on the assumption that the composite is linearly elastic. As we have mentioned above, if $\tau_f^c = k^c$, eqn (4.10) is identical to eqn (2.4) (Budiansky, 1983) for a perfectly plastic composite. In fact it is not necessary to limit this analysis to a perfectly plastic composite. We may extend it to a composite of bilinear response in shear using a different interpretation. A typical bilinear shear response of a strain-hardening composite with initial shear modulus G and tangent shear modulus $G'(0 < G' < G)$ after yielding is shown in Fig. 5. At the yield point γ_y there is a discontinuity in the tangent modulus. Let us introduce a short curve to smooth out the yield point. The following expression is assumed to hold within the short curve.

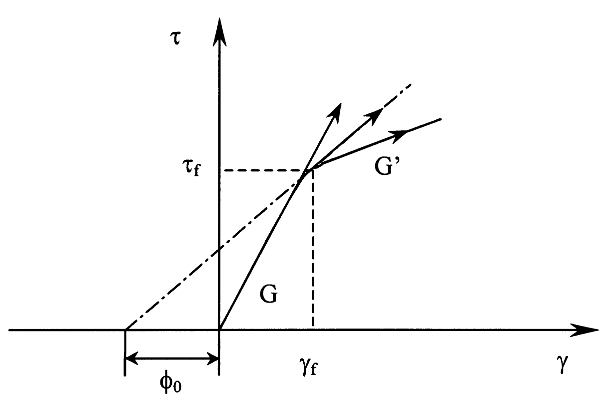

Fig. 5. Shear stress–strain curve of a shear strain hardening composite under compression.

$$\sigma_1 = \frac{\tau}{\gamma + \phi_0} \tag{7.1}$$

The necessary condition for a maximum σ_1 is

$$\frac{d\sigma_1}{d\gamma} = \frac{d}{d\gamma}\left(\frac{\tau}{\gamma + \phi_0}\right) = 0 \tag{7.2}$$

or equivalently,

$$\frac{d\tau}{d\gamma} = \frac{\tau_f}{\gamma_f + \phi_0} \tag{7.3}$$

At the tangent point, as shown in Fig. 5, σ_1 will achieve its maximum value, which is given by eqn (4.10). In the limiting case, there is no difference between τ_f and k, and we will get eqn (2.4). An additional constraint for this analysis is

$$G' \leqslant \frac{\tau_f}{\gamma_f + \phi_0} \tag{7.4}$$

Otherwise, eqn (4.10) will not give the maximum value. This argument can also be applied to eqn (5.16). However, a general shear strain-hardening composite needs to be assumed in the method of split rigidities. Procedures for finding snap buckling are explained by Budiansky and Fleck (1993), Harberle and Matthews (1994), Soutis and Turkmen (1995) and Daniel et al. (1996).

A more complete analysis of the kinking mechanism must include the effect of axial stress on transverse shear stress–strain relationship. For example, Hayashi (1985) found that shear strain–stress relation of epoxy resins depends on the compressive stress. Unfortunately, this effect has not been fully investigated. In Budiansky (1983) axial compressive stress is not included in the matrix yield condition for a perfectly plastic matrix. Recently Budiansky and Fleck (1993) have concluded that the assumption of axially rigid fibers is well justified in their kinking analysis. However, more recently, experimental results (Soutis and Turkmen, 1995; Kyriakides et al., 1995; Daniel et al., 1996; Vogler and Kyriakides, 1997; Kyriakides and Ruff, 1997; and Soutis, 1997; Moran and Shih, 1998) showed that the initiation of a kink band was sudden and occurred at axial strain levels of around 1%. Interestingly, the shear yield stress of a polymeric matrix is also close to this strain value (Jelf and Fleck, 1992). This means that the axial normal compressive strain is at least of the same order as the perturbed shear strain when the kink band occurs, and the axial compressive stress plays a significant role in the formation of a kink band.

Therefore, it seems a yield criterion along the lines suggested by Hahn (1987) and Williams and Cairns (1994) should be applied. No accounting for a possible shear stress concentration the Tresca criterion in a two-dimensional model gives,

$$k^c = \tau_f^c = \tau_f^m = \sqrt{(k^m)^2 - \tfrac{1}{4}\left(\sigma_1^m\right)^2} < k^m \tag{7.5}$$

The von Mises criterion gives the same expression with 1/3 instead of 1/4. We may note that the interfacial shear strength, k^c, is generally not a material constant. Using the axial isostrain condition to express the compressive stress in the matrix in terms of the composite axial stress and inserting it in eqn (7.5) and on substitution in eqn (4.10) gives,

$$\sigma_1^c = \frac{G_{13}^c}{1 + G_{13}^c\phi_0 \Big/ \sqrt{(k^m)^2 - \frac{1}{4}\left(\frac{E^m\sigma_1^c}{E_1^c}\right)^2}} \tag{7.6}$$

Equation (7.6) is generally not easy to apply. However, from the Tresca criterion, if

$$\sigma_1^c \ll 2\frac{E_1^c k^m}{E^m} = \frac{E_1^c \sigma_y^m}{E^m} = \sigma_y^c \tag{7.7}$$

eqn (7.5) simplifies as

$$k^c = \tau_f^c \cong k^m \tag{7.8}$$

Equation (7.6) then becomes

$$\sigma_1^c = \frac{k^m}{\gamma_y^c + \phi_0} \tag{7.9}$$

This means that eqn (7.9) can only give an accurate kinking stress if the axial stress is much less than the yielding stress. The condition in eqn (7.7) is derived using the Tresca criterion, and it may not be a good estimate to use in eqn (7.6). Alternatively, eqn (7.6) can be rewritten as

$$\sigma_1^c = \frac{k^m}{\sqrt{\left(\gamma_y^c + \phi_0\right)^2 + \frac{1}{4}\left(\frac{E^m}{E_1^c}\right)^2}} \tag{7.10}$$

if E^m/E_1^c is very small, eqn (7.10) reduces to (7.9). A rough estimate is to let $\gamma_y^c + \phi_0$ be 0.05 (about 3° in Jelf and Fleck, 1992), and

$$\frac{E_1^c}{E^m} = v^f \frac{E^f}{E^m} > 22 \text{ (25 in the von Mises criterion)} \tag{7.11}$$

to keep an estimation error in eqn (7.9) less than 10%. Under this condition, the rigid-fiber assumption (Budiansky and Fleck, 1993) is acceptable.

Equations (2.4) and (7.9) cannot be compared directly because k^c and k^m are two different material measurements. In eqn (2.4) k^c is the interfacial shear strength that may not be a material constant, and in eqn (7.9) k^m is the shear yield stress of the matrix. In the literature, however, this difference is not clearly recognized (e.g., Jelf and Fleck, 1992). Under the condition of eqn (7.7), the meanings of k^c and k^m may be only slightly different. However, γ_y^c and γ_y^m are always distinguishable. With eqn (7.7), $y_y^c \cong (1 - v^f)\gamma_y^m$ using eqn (3.14) for a composite with shear-stiff fibers. Therefore,

$$\frac{k^m}{\gamma_y^m + \phi_0} < \sigma_1^c = \frac{k^m}{\gamma_y^c + \phi_0} < \frac{k^m}{\phi_0} \tag{7.12}$$

Generally speaking, Argon's result (1972) is always an upper bound to eqn (7.9), and Budiansky's result (1983) is a lower bound if the interfacial shear strength of the composite is interpreted as the shear yield stress of the matrix.

In another extreme case, when fibers are nearly perfectly aligned, $\gamma_y^c + \phi_0$ must be very small. Equation (7.10) then becomes

$$\sigma_1^c \cong 2\frac{E_1^c k^m}{E^m} = \frac{E_1^c \sigma_y^m}{E^m} \tag{7.13}$$

which relates the composite compressive strength to the matrix yield stress according to the Tresca criterion. This is consistent with the theory of shear instability of matrix in Section 6. We also need to point out that the assumption of axially rigid fibers is not justified if $\gamma_y^c + \phi_0$ is very small.

The fiber–matrix interfacial debonding is another issue to be considered here. According to Lanir and Fung (1972), assuming the bond strength to be zero, separation will occur if the normal stress in the interface vanishes. Therefore, if Poisson's ratio $\nu^f < \nu^m$, separation will occur in compression. Poisson's ratio ν^f is difficult to measure, and no experimental data for this property are available in the literature. Most often $\nu^f = 0.3$ is taken. Poisson's ratio of the matrix in the elastic regime can differ depending on the polymeric material, but it will always approach 0.5 when the matrix yields. A rough assumption is that the interfacial debonding will exist if the matrix yields in compression. With this hypothesis, the analysis presented above for matrix yielding will also be valid for the case of interfacial debonding.

8. Conclusions

As a general conclusion of the analyses presented in this paper it may be stated that in the compressive failure of fiber reinforced composites, which is complex and multi-modal, the shear deformation of fibers and matrix play key roles. From the microbuckling and kink band analyses performed here, with emphasis on the shear behavior, following results may be summarized.

In the elastic microbuckling analysis, a new shear deformation beam model has been developed for a two-dimensional periodic matrix–fiber–matrix, and the general Rosen microbuckling formula in eqn (3.24) has been proved as a consequence. In the elastic–plastic microbuckling analysis accounting for the fiber misalignment waviness, the Argon–Budiansky kinking formula has been obtained. This analysis unifies the microbuckling and kink band analyses into a single model. By virtue of the assumed uniform shear strains in the model, the shear modulus of the composite follows the 'inverse rule of mixtures', and is the Reuss lower bound of the effective shear modulus.

In the macrobuckling model, a 'shear hinge' has been proposed to simulate the kink band based on the method of split rigidities. Both the Rosen formula and the Argon–Budiansky formula have been shown to result also from this model. It has been further shown that not only initial fiber misalignment but also misinclination of loading are important parameters in the kinking analysis. The analysis helps explain that even in a composite with perfectly straight fibers a kink band is possible.

A new theory of shear instability of fiber reinforced composites in compression has been developed based on the mechanism of matrix shear sliding (plastic) deformation and fiber microbuckling. Unlike other theories that treat the fiber–matrix system as an equivalent anisotropic medium, this theory explicitly includes the constituent properties. A simple expression for the kink band angle in terms of the fiber volume fraction has been derived, and it may be a reasonable upper bound estimate.

In the micromechanical model it has been shown that the interfacial shear strength of the composite is not a material constant, if the axial compressive stress cannot be neglected. A modification has been introduced to the Argon–Budiansky kinking formula based on the yield criterion of the matrix combining axial compressive stress and transverse shear stress. The Argon–Budiansky kinking formula, with a different interpretation, has been shown to result from this model having initial fiber misalignment if the axial compressive stress is relatively small of if the ratio of fiber modulus to matrix modulus is very large. For a nearly perfect system, the kinking compression strength has been shown to relate to the matrix yield stress according to the Tresca criterion.

Appendix

For the two-dimensional model shown in Fig. 1(a) or (b), due to the symmetric or antisymmetric geometry, a representative element consists of one layer of fiber (height $H^{\rm f}$) bounded by the two adjacent matrix materials (height $H^{\rm m}$). The instability is predicted by the governing equation of the fiber considering perturbations about the equilibrium state. The buckling equation of the fiber is

$$D^{\rm f}\frac{{\rm d}^4 w^{\rm f}}{{\rm d}x^4}+\frac{\rm d}{{\rm d}x}\left(P^{\rm f}\frac{{\rm d}w^{\rm f}}{{\rm d}x}\right)-q^{\rm f}+\frac{{\rm d}m^{\rm f}}{{\rm d}x}=0 \tag{A.1}$$

A.1. Extensional mode

For Fig. 1(a) the Rosen (1965) assumptions in extensional mode are $m^{\rm f}=0$, i.e., no shear stress moment, and

$$q^{\rm f}=-k^{\rm m}w^{\rm f}=-2\frac{E^{\rm m}}{H^{\rm m}}w^{\rm f} \tag{A.2}$$

where $k^{\rm m}$ is the stiffness of the matrix (as the elastic foundation). Thus, Rosen's extensional mode is for a beam embedded into the Winkler foundation. For the fiber pinned at both ends, the general solution of eqn (A.1) is

$$w^{\rm f}=a_n\sin\frac{n\pi x}{L} \tag{A.3}$$

and the buckling load is

$$P^{\rm f}=\frac{\pi^2E^{\rm f}I^{\rm f}}{L^2}\left(n^2+\frac{2E^{\rm m}L^4}{n^2H^{\rm m}\pi^4E^{\rm f}I^{\rm f}}\right) \tag{A.4}$$

If L is long enough, n is considered to be a continuous variable, and minimization of $P^{\rm f}$ with respect to n^2 yields

$$n_{\rm cr}^2=\sqrt{\frac{2E^{\rm m}L^4}{H^{\rm m}\pi^4E^{\rm f}I^{\rm f}}} \tag{A.5}$$

and

$$P_{\rm cr}^{\rm f}=2\sqrt{k^{\rm m}E^{\rm f}I^{\rm f}}=2\sqrt{\frac{2E^{\rm m}E^{\rm f}I^{\rm f}}{H^{\rm m}}} \tag{A.6}$$

If the compressive force in the matrix is negligible, the critical compressive stress of the composite for extensional mode in the longitudinal direction is as follows (Rosen, 1965)

$$\sigma_1^{\rm c}=v^{\rm f}\frac{P^{\rm f}}{H^{\rm f}}=2\frac{v^{\rm f}}{H^{\rm f}}\sqrt{\frac{2E^{\rm m}E^{\rm f}I^{\rm f}}{H^{\rm m}}}=2v^{\rm f}\sqrt{\frac{v^{\rm f}E^{\rm m}E^{\rm f}}{3(1-v^{\rm f})}} \tag{A.7}$$

If the boundary constraint at one of the fiber end is free, the fiber can be treated as a semi-infinite beam (or an infinite beam). The buckling stress becomes

$$\sigma_1^c = v^f \sqrt{\frac{v^f E^m E^f}{3(1 - v^f)}} \tag{A.8}$$

which is only one-half of the value obtained from eqn (A.7).

It is worth point out that Rosen's analysis for the extensional mode neglects shear deformation in the matrix because $m^f = 0$ is assumed. In fact, if the buckling perturbation normal displacement of the matrix u^m is assumed as a function of x only, on either side of the fiber, the shear strain of the matrix just near the interface of the fiber is

$$\gamma_{13}^m = \frac{\partial w^m}{\partial x} + \frac{\partial u^m}{\partial z} = \frac{\partial w^m}{\partial x} = \frac{\partial w^f}{\mathrm{d}x} \tag{A.9}$$

Also, traction is continuous on the interface,

$$\tau_{13}^f = \tau_{13}^m = G^m \gamma_{13}^m = G^m \frac{\mathrm{d}w^f}{\mathrm{d}x} \tag{A.10}$$

For the extensional mode the distributed moment in eqn (A.1) due to surface shear stress is

$$m^f = -H^f \tau_{13}^f \tag{A.11}$$

The buckling equation of the fiber now becomes (Xu and Reifsnider, 1993, 1994)

$$D^f \frac{\mathrm{d}^4 w^f}{\mathrm{d}x^4} + (P^f - G^m H^f) \frac{\mathrm{d}^2 w^f}{\mathrm{d}x^2} + k^m w^f = 0 \tag{A.12}$$

and the critical stress

$$\sigma_1^c = v^f \left[2\sqrt{\frac{v^f E^m E^f}{3(1 - v^f)}} + G^m \right] \tag{A.13}$$

which predicts a higher critical composite stress compared to eqn (A.7). The compressive force in the matrix can be included by introducing the 'rule of mixtures' as follows

$$\sigma_1^c = \frac{v^f E^f + (1 - v^f) E^m}{E^f} \left(2\sqrt{\frac{v^f E^m E^f}{2(1 - v^f)}} + G^m \right) \tag{A.14}$$

A.2. Shear mode

Since all fibers deform exactly the same way in the shear mode, as shown in Fig. 1(b), the composite constituent displacement fields are uniform and antisymmetric with respect to the x coordinate. A representative element of the composite is similar to the extensional mode. Since there is no lateral extension or compression in the matrix, a normal distributed load can be assumed as [comparing with eqn (A.2)]

$$q^f = 0 \tag{A.15}$$

If the fiber shear deformation is negligible, the matrix shear strain is as (in Fig. 2)

$$\gamma_{13}^{\mathrm{m}} = \frac{\partial w^{\mathrm{m}}}{\partial x} + \frac{\partial u^{\mathrm{m}}}{\partial z} = \frac{\mathrm{d}w^{\mathrm{f}}}{\mathrm{d}x} + \frac{H^{\mathrm{f}}}{2H^{\mathrm{m}}}\frac{\mathrm{d}w^{\mathrm{f}}}{\mathrm{d}x} = \frac{1}{1-v^{\mathrm{f}}}\frac{\mathrm{d}w^{\mathrm{f}}}{\mathrm{d}x} \tag{A.16}$$

Unlike non-uniform shear strain in the extensional mode, γ_{13}^{m} is uniformly distributed in the whole matrix in the lateral direction. Substitution of eqn (A.16) and eqn (A.11) into eqn (A.1) yields the buckling equation of the fiber in the shear mode as

$$D^{\mathrm{f}}\frac{\mathrm{d}^4 w^{\mathrm{f}}}{\mathrm{d}x^4} + \left(P^{\mathrm{f}} - \frac{G^{\mathrm{m}}H^{\mathrm{f}}}{1-v^{\mathrm{f}}}\right)\frac{\mathrm{d}^2 w^{\mathrm{f}}}{\mathrm{d}x^2} = 0 \tag{A.17}$$

Assuming L is very large, the critical compressive stress is (Hahn and Williams, 1986)

$$\sigma_1^{\mathrm{c}} = v^{\mathrm{f}}\frac{P^{\mathrm{f}}}{H^{\mathrm{f}}} = \frac{v^{\mathrm{f}}}{1-v^{\mathrm{f}}}G^{\mathrm{m}} \tag{A.18}$$

If we add shear stress acting in the matrix, but do not account for the matrix bending stiffness, i.e., $D^{\mathrm{m}} = 0$, the moment in the representative element of the composite becomes

$$m^{\mathrm{c}} = -H^{\mathrm{f}}\tau_{13}^{\mathrm{f}} - 2H^{\mathrm{m}}\tau_{13}^{\mathrm{m}} = -\left(H^{\mathrm{f}} + 2H^{\mathrm{m}}\right)\tau_{13}^{\mathrm{m}} \tag{A.19}$$

or, as in an alternative treatment (Sun and Jun, 1993)

$$m^{\mathrm{f}} = -H^{\mathrm{f}}\tau_{13}^{\mathrm{f}} \tag{A.20}$$

and

$$q^{\mathrm{f}} = 2H^{\mathrm{m}}\frac{\mathrm{d}\tau_{13}^{\mathrm{m}}}{\mathrm{d}x} = 2\frac{H^{\mathrm{m}}G^{\mathrm{m}}}{1-v^{\mathrm{f}}}\frac{\mathrm{d}^2 w^{\mathrm{f}}}{\mathrm{d}x^2} \tag{A.21}$$

Now the buckling equation can be rewritten as

$$D^{\mathrm{f}}\frac{\mathrm{d}^4 w^{\mathrm{f}}}{\mathrm{d}x^4} + \left[P^{\mathrm{f}} - \frac{G^{\mathrm{m}}H^{\mathrm{f}}}{v^{\mathrm{f}}(1-v^{\mathrm{f}})}\right]\frac{\mathrm{d}^2 w^{\mathrm{f}}}{\mathrm{d}x^2} = 0 \tag{A.22}$$

For the fiber pinned at both ends, the critical buckling load is

$$P^{\mathrm{f}} = \frac{H^{\mathrm{f}}}{v^{\mathrm{f}}(1-v^{\mathrm{f}})}G^{\mathrm{m}} + \frac{\pi^2 E^{\mathrm{f}} I^{\mathrm{f}}}{L^2} \tag{A.23}$$

For the fiber clamped at both ends, the critical buckling load is

$$P^{\mathrm{f}} = \frac{H^{\mathrm{f}}}{v^{\mathrm{f}}(1-v^{\mathrm{f}})}G^{\mathrm{m}} + \frac{4\pi^2 E^{\mathrm{f}} I^{\mathrm{f}}}{L^2} \tag{A.24}$$

For the fiber free at both ends, the critical buckling load is

$$P^{\mathrm{f}} = \frac{H^{\mathrm{f}}}{v^{\mathrm{f}}(1-v^{\mathrm{f}})}G^{\mathrm{m}} \tag{A.25}$$

It is easy to see from eqns (A.23)–(A.25) that if the fiber length L is large enough all three boundary conditions will give the same buckling load. Now the well-known Rosen's solution (1965) is obtained as

$$\sigma_1^{\mathrm{c}} = v^{\mathrm{f}} \frac{P^{\mathrm{f}}}{H^{\mathrm{f}}} = -\frac{1}{1 - v^{\mathrm{f}}} G^{\mathrm{m}} \tag{A.26}$$

A.3. Misalignment defects

An initial transverse fiber misalignment w_0^{f} is assumed to be

$$w_0^{\mathrm{f}} = a_0 \sin \frac{n\pi x}{L} \tag{A.27}$$

where a_0 is assumed to be very small, and has no major effect on what we have developed above. The buckling equation of the fiber is modified as

$$D^{\mathrm{f}} \frac{\mathrm{d}^4 w^{\mathrm{f}}}{\mathrm{d}x^4} + \frac{\mathrm{d}}{\mathrm{d}x}\left[P^{\mathrm{f}} \frac{\mathrm{d}\left(w^{\mathrm{f}} + w_0^{\mathrm{f}}\right)}{\mathrm{d}x}\right] - q^{\mathrm{f}} + \frac{\mathrm{d}m^{\mathrm{f}}}{\mathrm{d}x} = 0 \tag{A.28}$$

where w^{f} is interpreted as an increment of the transverse displacement.

In the shear mode, a particular solution in eqn (A.28) is assumed as eqn (A.3) for the fiber pinned at both ends, and then

$$P^{\mathrm{f}} = \frac{a_n}{a_n + a_0}\left[\left(H^{\mathrm{f}} + 2H^{\mathrm{m}}\right)\frac{G^{\mathrm{m}}}{1 - v^{\mathrm{f}}} + E^{\mathrm{f}} I^{\mathrm{f}} \left(\frac{n\pi}{L}\right)^2\right] \tag{A.29}$$

Again, if the second term is negligible, a simple relation is obtained as

$$\sigma_1^{\mathrm{c}} = \frac{E_1^{\mathrm{c}} \sigma_1^{\mathrm{f}}}{E^{\mathrm{f}}} \cong \frac{a_n}{a_n + a_0} \frac{G^{\mathrm{m}}}{1 - v^{\mathrm{f}}} \cong \frac{a_n}{a_n + a_0} G_{13}^{\mathrm{c}} \tag{A.30}$$

References

Argon, A., 1972. Fracture of composites. In: Herman, H. (Ed.), Treatise on Materials Science and Technology, vol. 1. Academic Press, New York, pp. 79–114.

Bijlaard, P.P., 1951. Analysis of the elastic and plastic stability of sandwich plates by the method of split rigidities—I. Journal of Aeronautical Sciences 18, 339–349.

Budiansky, B., 1974. Theory of buckling and post-buckling behavior of elastic structures. In: Yih, C.S. (Ed.), Advances in Applied Mechanics, vol. 14. Academic Press, New York, pp. 1–65.

Budiansky, B., 1983. Micromechanics. Computers and Structures 16, 3–12.

Budiansky, B., Fleck, N.A., 1993. Compressive failure of fiber composites. J. Mechanics Phys. Solids 41, 183–211.

Budiansky, B., Fleck, N.A., Amazigo, J.C., 1998. On kink-band propagation in fiber composites. J. Mechanics Phys. Solids 46, 1637–1653.

Camponeschi Jr., E.T., 1991. Compression of composite materials: a review. In: O'Brien, T.K. (Ed.), Composite Materials: Fatigue and Fracture, vol. 3. ASTM STP 1110, Philadelphia, PA, pp. 550–578.

Chaudhuri, R.A., 1991. Prediction of the compressive strength of thick-section advanced composite laminates. J. of Composite Materials 25, 1244–1276.

Chou, T.W., Kelly, A., 1980. The effect of transverse shear on the longitudinal compressive strength of fiber composites. J. of Materials Science 15, 327–331.

Christensen, R.M., DeTeresa, S.J., 1997. The kink band mechanism for the compressive failure of fiber composite materials. J. of Applied Mechanics 64, 1–6.

Christoffersen, J., Jensen, H.M., 1996. Kink band analysis accounting for the microstructure of fiber reinforced materials. Mechanics of Materials 24, 305–315.

Chung, I., Weitsman, Y., 1994. A mechanics model for the compressive response of fiber reinforced composites. Int. J. Solids Structures 31, 2519–2536.

Chung, I., Weitsman, Y., 1995. On the buckling/kinking compressive failure of fibrous composites. Int. J. Solids Structures 32, 2329–2344.

Daniel, I.M., Hsiao, H.M., Wooh, S.C., 1996. Failure mechanisms in thick composites under compressive loading. Composites, Part B 27B, 543–552.

Deve, H.E., 1997. Compressive strength of continuous fiber reinforced aluminium matrix composites. Acta Mater 45, 5041–5046.

Fleck, N.A., 1997. Compressive failure of fiber composites. In: Hutchinson, J.W., Wu, T.Y. (Eds.), Advances in Applied Mechanics, vol. 33. Academic Press, New York, pp. 47–117.

Foye, R.L., 1966. Compression strength of unidirectional composites. AIAA Paper No. 66–143.

Greszczuk, L.B., 1974. Microbuckling of lamina-reinforced composites. Composite Materials: Testing and Design (Third Conference), ASTM STP 546, Philadelphia, PA, pp. 5–29.

Hahn, H.T., 1987. Compressive failure of unidirectional composites. International Symposium for Testing and Failure Analysis, ISTFA, 1987. ASM, Metals Park, Ohio, pp. 235–238.

Hahn, H.T., Williams, J.G., 1986. Compression failure mechanisms in unidirectional composites. In: Whitney, J.M. (Ed.), Composite Materials: Testing and Design (Seventh Conference). ASTM STP 893, Philadelphia, PA, pp. 115–139.

Harberle, J.G., Matthews, F.L., 1994. A micromechanics model for compressive failure of unidirectional fiber-reinforced plastics. J. of Composite Materials 28, 1618–1639.

Hayashi, T., 1985. Shear modulus of epoxy resin under compression. In: Vinson, J.R., Taya, M. (Eds.), Recent Advances in Composites in the United States and Japan. ASTM STP 864, Philadelphia, PA, pp. 676–684.

Hsu, S.-Y., Vogler, T.J., Kyriakides, S., 1998. Compressive strength predictions for fiber composites. J. of Applied Mechanics 65, 7–16.

Hu, H., 1984. Variational Principles of Theory of Elasticity with Applications. Science Press, Beijing.

Jelf, P.M., Fleck, N.A., 1992. Compression failure mechanisms in unidirectional composites. J. of Composite Materials 26, 2706–2726.

Jensen, H.M., Christoffersen, J., 1997. Kink band formation in fiber reinforced materials. J. Mech. Phys. Solids 45, 1121–1136.

Kulkarni, S.V., Rice, J.S., Rosen, B.W., 1975. An investigation of the compressive strength of kevlar 49/epoxy composites. Composites 3, 217–225.

Kyriakides, S., Ruff, A.E., 1997. Aspects of the failure and postfailure of fiber composites in compression. J. of Composite Materials 31, 2000–2037.

Kyriakides, S., Arseculeratne, R., Perry, E.J., Liechti, K.M., 1995. On the compressive failure of fiber reinforced composites. Int. J. Solids Structures 32, 689–738.

Lanir, Y., Fung, Y.C.B., 1972. Fiber composite columns under compression. J. Composite Materials 6, 387–401.

Moran, P.M., Shih, C.F., 1998. Kink band propagation and broadening in ductile matrix fiber composite: experiments and analysis. Int. J. Solids Structures 35, 1709–1722.

Moran, P.M., Liu, X.H., Shih, C.F., 1995. Kink band formation and band broadening in fiber composites under compressive loading. Acta Metall. Mater 43, 2943–2958.

Niu, K., Talreja, R., 1998. Modeling of wrinkling in sandwich panels under compression, to appear in J. Engineering Mechanics.

Parton, V.Z., Kudryavtsev, B.A., 1998. Engineering Mechanics of Composite Structures. CRC Press, Boca Raton, FL.

Rosen, V.W., 1965. Mechanics of composite strengthening. In: Fiber Composite Materials. American Society of Metals, Metals Park, Ohio, pp. 37–75.

Schadler, L., 1998. Private communication.

Schapery, R.A., 1995. Prediction of compressive strength and kink bands in composites using a work potential. Int. J. Solids Structures 32, 739–765.

Schultheisz, C.R., Waas, A.M., 1996. Compressive failure of composites, Part I: testing and micromechanical theories. Progress in Aerospace Sciences 32, 1–42.

Soutis, C., 1997. Compressive strength of unidirectional composites: measurement and prediction. In: Hooper, S.J. (Ed.), Composite Materials: Testing and Design, vol. 13. ASTM STP 1242, Philadelphia, PA, pp. 168–176.

Soutis, C., Turkmen, D., 1995. Influence of shear properties and fiber imperfections on the compressive behavior of gfrp laminates. Applied Composite Materials 2, 327–342.

Stief, P.S., 1987. An exact two-dimensional approach to fiber micro-buckling. Int. J. Solids Structures 23, 1235–1246.

Stief, P.S., 1988. A simple model for the compressive failure of weakly bonded, fiber-reinforced composites. J. of Composite Materials 22, 818–828.

Steif, P.S., 1990. A model for kinking in fiber composite–II kink band formation. Int. J. Solids Structures 26, 563–569.

Sun, C.T., Jun, A.W., 1993. Effect of matrix nonlinear behavior on the compressive strength of fiber composites. In: Rajapakse, Y.D.S. (Ed.), Mechanics of Thick Composites. ASME, New York, pp. 91–105.

Tomblin, J.S., Barbero, E.J., Godoy, L.A., 1997. Imperfection sensitivity of fiber microbuckling in elastic–nonlinear polymer-matrix composites. Int. J. Solids Structures 34, 1667–1679.

Vogler, T.J., Kyriakides, S., 1997. Initiation and axial propagation of kink bands in fiber composites. Acta Mater. 45, 2443–2454.

Waas, A.M., Babcock Jr., C.D., Knauss, W.G., 1990. A mechanical model for elastic fiber microbuckling. J. of Applied Mechanics 57, 138–149.

Wang, A.S.D., 1978. A non-linear microbuckling model predicting the compressive strength of unidirectional composites. In: ASME Winter Annual Meeting, ASME Paper 78-WA/Aero-1.

Williams, T.O., Cairns, D.S., 1994. A model for the compressive failure of composite materials. J. of Composite Materials 28, 92–111.

Wisnom, M.R., 1990. The effect of fiber misalignment on the compressive strength of unidirectional carbon fibre/epoxy. Composites 21, 403–407.

Xu, Y.L., Reifsnider, K.L., 1993. Micromechanical modeling of composite compressive strength. J. of Composite Materials 27, 558–572.

Xu, Y.L., Reifsnider, K.L., 1994. Composite compressive strength prediction using a nonhomogeneous foundation model. In: Groves, S.E., Highsmith, A.L. (Eds.), Compression Response of Composite Structures. ASTM, STP 1185, Philadelphia, PA, pp. 306-319.

Yeh, J.R., Teply, J.L., 1988. Compressive response of kevlar/epoxy composites. J. of Composite Materials 22, 245–257.

Zhang, G., Latour Jr., R.A., 1994. An analytical and numerical study of fiber microbuckling. Composite Science and Technology 51, 95–109.